

Folding Mechanisms of Entangled Proteins

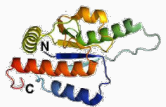
Numerical studies within coarse-grained
structure-based models

Leonardo Salicari | `leonardo.salicari@phd.unipd.it`

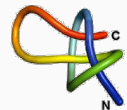
University of Padua, Department of Physics and Astronomy



3_1 Knot



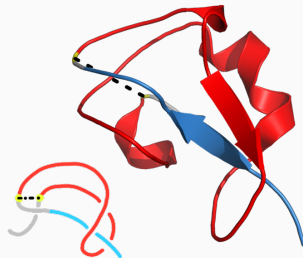
Slipknot





$$G'(i, j) = \frac{1}{4\pi} \sum_{i=i_1}^{i_2-1} \sum_{j=j_1}^{j_2-1} \frac{\mathbf{R}_i - \mathbf{R}_j}{|\mathbf{R}_i - \mathbf{R}_j|^3} \cdot (\Delta\mathbf{R}_i \times \Delta\mathbf{R}_j)$$

Type III Antifreeze protein RD1

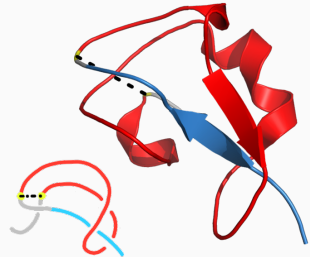


32% of proteins domains contains at least one *entangled loop* motif



$$G'(i, j) = \frac{1}{4\pi} \sum_{i=i_1}^{i_2-1} \sum_{j=j_1}^{j_2-1} \frac{\mathbf{R}_i - \mathbf{R}_j}{|\mathbf{R}_i - \mathbf{R}_j|^3} \cdot (\Delta \mathbf{R}_i \times \Delta \mathbf{R}_j)$$

Type III Antifreeze protein RD1



32% of proteins domains contains at least one *entangled loop* motif



- Entangled loops enriched in the C-terminal side of the entanglement they are in
- high $|G'|$ contacts tend to be weakly bounded

Hypothesis

Contacts with high $|G'|$ tend to form in the later stages of the folding



- Entangled loops enriched in the C-terminal side of the entanglement they are in
- high $|G'|$ contacts tend to be weakly bounded

Hypothesis

Contacts with high $|G'|$ tend to form in the later stages of the folding



- Entangled loops enriched in the C-terminal side of the entanglement they are in
- high $|G'|$ contacts tend to be weakly bounded

Hypothesis

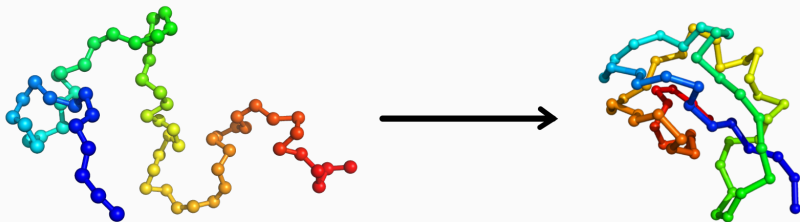
Contacts with high $|G'|$ tend to form in the later stages of the folding



Goal

Use MD to sample folding events of a protein having an entangled loop in its native state.
Is the formation of contacts with high $|G'|$ postponed?

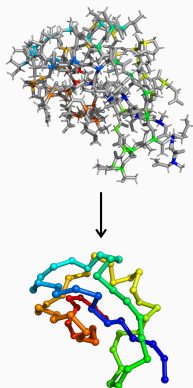
Type III Antifreeze Protein RD1 (PDB: 1UCS)



Ko, Tzu-Ping *et al.*; *Biophys. J* (2003) | García-Arribas, O. *et al.*; *Protein Sci.* (2007) | Kundu, S. *et al.*; *J. Mol. Graph. Model.* (2008) | Chen, H. L. *et al.*; *Proteins* (2010)

The model

Alpha Carbon Rep



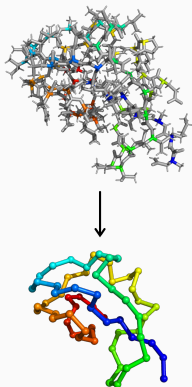
Structure-based

$$\begin{aligned}
 v = & \sum_{i=1}^{N-1} \epsilon_r^i (r^i - r_o^i)^2 \\
 & + \sum_{i=1}^{N-2} \epsilon_\theta^i (\theta^i - \theta_o^i)^2 \\
 & + \sum_{i=1}^{N-3} \epsilon_\phi^i \{ [1 - \cos(\phi^i - \phi_o^i)] \\
 & + \frac{1}{2} [1 - \cos(3(\phi^i - \phi_o^i))] \} \\
 & + \sum_{i=1}^N \sum_{j=1}^N 4\epsilon_C^{ij} \left[\left(\frac{\sigma^{ij}}{\Delta r^{ij}} \right)^{12} - \left(\frac{\sigma^{ij}}{\Delta r^{ij}} \right)^6 \right] \\
 & + \sum_{i=1}^N \sum_{j=1}^N \epsilon_{NN}^{ij} \left(\frac{\sigma_{NN}^{ij}}{\Delta r^{ij}} \right)^{12}
 \end{aligned}$$

Langevin Dynamics

$$m_i \frac{d^2 \vec{r}^i}{dt^2} = -\gamma \frac{d\vec{r}^i}{dt} - \nabla V + \vec{R}^i$$

Alpha Carbon Rep



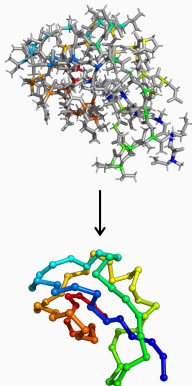
Structure-based

$$\begin{aligned}
 V = & \sum_{i=1}^{N-1} \epsilon_r^i (r^i - r_o^i)^2 \\
 & + \sum_{i=1}^{N-2} \epsilon_\theta^i (\theta^i - \theta_o^i)^2 \\
 & + \sum_{i=1}^{N-3} \epsilon_\phi^i \{ [1 - \cos(\phi^i - \phi_o^i)] \\
 & + \frac{1}{2} [1 - \cos(3(\phi^i - \phi_o^i))] \} \\
 & + \sum_{i=1}^N \sum_{j=1}^N 4\epsilon_C^{ij} \left[\left(\frac{\sigma^{ij}}{\Delta r^{ij}} \right)^{12} - \left(\frac{\sigma^{ij}}{\Delta r^{ij}} \right)^6 \right] \\
 & + \sum_{i=1}^N \sum_{j=1}^N \epsilon_{NN}^{ij} \left(\frac{\sigma_{NN}^{ij}}{\Delta r^{ij}} \right)^{12}
 \end{aligned}$$

Langevin Dynamics

$$m_i \frac{d^2 \vec{r}^i}{dt^2} = -\gamma \frac{d\vec{r}^i}{dt} - \nabla V + \vec{R}^i$$

Alpha Carbon Rep



Structure-based

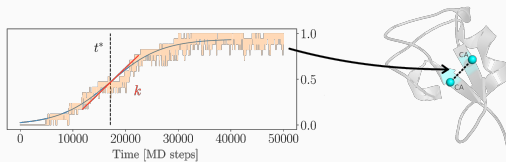
$$\begin{aligned}
 v = & \sum_{i=1}^{N-1} \epsilon_r^i (r^i - r_o^i)^2 \\
 & + \sum_{i=1}^{N-2} \epsilon_\theta^i (\theta^i - \theta_o^i)^2 \\
 & + \sum_{i=1}^{N-3} \epsilon_\phi^i \{ [1 - \cos(\phi^i - \phi_o^i)] \\
 & + \frac{1}{2} [1 - \cos(3(\phi^i - \phi_o^i))] \} \\
 & + \sum_{i=1}^N \sum_{j=1}^N 4\epsilon_C^{ij} \left[\left(\frac{\sigma^{ij}}{\Delta r^{ij}} \right)^{12} - \left(\frac{\sigma^{ij}}{\Delta r^{ij}} \right)^6 \right] \\
 & + \sum_{i=1}^N \sum_{j=1}^N \epsilon_{NN}^{ij} \left(\frac{\sigma_{NN}^{ij}}{\Delta r^{ij}} \right)^{12}
 \end{aligned}$$

Langevin Dynamics

$$m_i \frac{d^2 \vec{r}^i}{dt^2} = -\gamma \frac{d\vec{r}^i}{dt} - \nabla V + \vec{R}^i$$

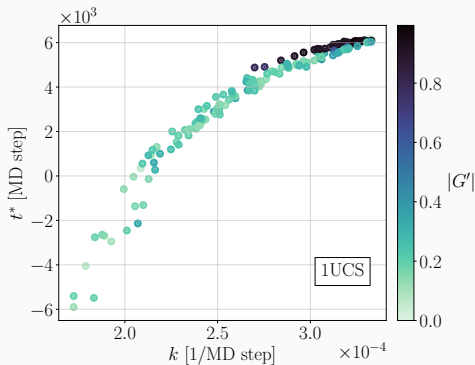
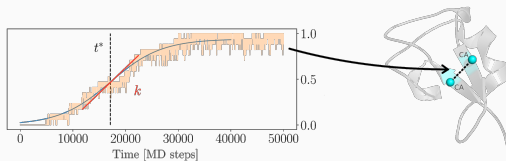
Results Contact formation time t^* and contact cooperativity k

Probability of contact formation

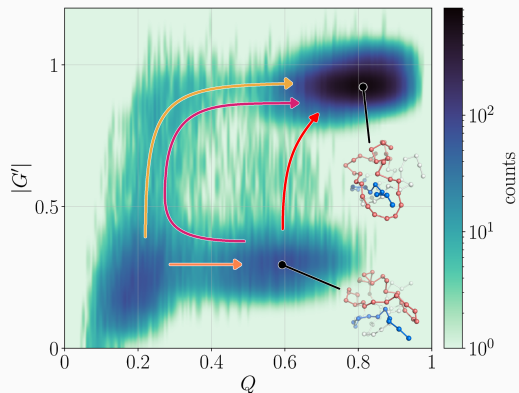


Results Contact formation time t^* and contact cooperativity k

Probability of contact formation

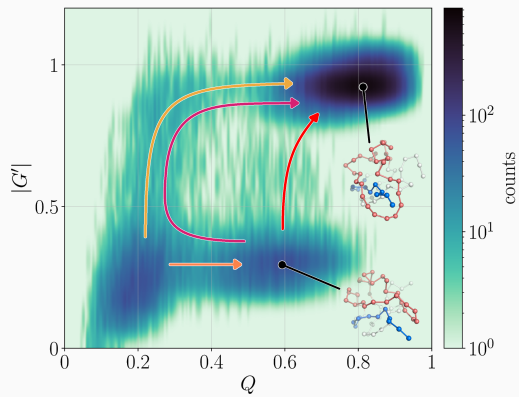


Results Trajectories along reaction coordinates



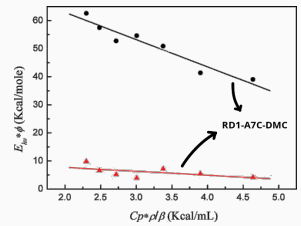
Folding Experiment

$$E_{hv\phi} = q + \Delta_R V \left(\frac{C_{DPF}}{\beta} \right)_T$$



Folding Experiment

$$E_{hv\phi} = q + \Delta_{RV} \left(\frac{C_{p\rho}}{\beta} \right)_T$$





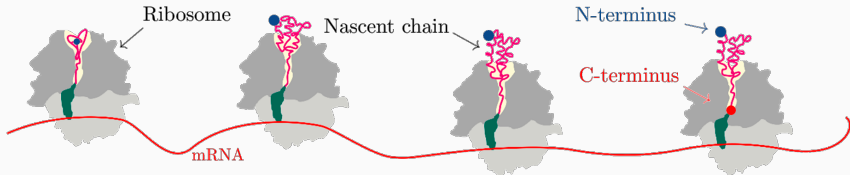
- Entangled loops enriched in the C-terminal side of the entanglement they are in
- high $|G'|$ contacts tend to be frustrated

Hypothesis

Contacts with high $|G'|$ tend to form in the later stages of the folding

Probing cotranslational events through:

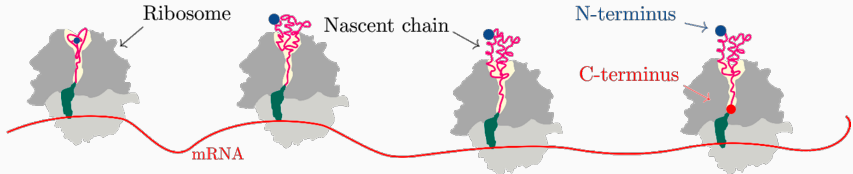
- MD coarse-grained simulations
- Statistical models: the Wako-Saitô-Muñoz-Eaton (WSME) model





Probing cotranslational events through:

- MD coarse-grained simulations
- Statistical models: the Wako-Saitô-Muñoz-Eaton (WSME) model



Appendix Example of Q and $|G'|$ timeseries

